0022-3565/01/2972-780–789$3.00
THE JOURNAL OF PHARMACOLOGY AND EXPERIMENTAL THERAPEUTICS
Copyright © 2001 by The American Society for Pharmacology and Experimental Therapeutics
JPET 297:780–789, 2001

Vol. 297, No. 2
3244/896000
Printed in U.S.A.

Structure-Hepatic Disposition Relationships for Cationic Drugs in Isolated Perfused Rat Livers: Transmembrane Exchange and Cytoplasmic Binding Process

DANIEL Y. HUNG, PING CHANG, MICHAEL WEISS, and MICHAEL S. ROBERTS

Department of Medicine, University of Queensland, Princess Alexandra Hospital, Woolloongabba, Queensland, Australia (D.Y.H., P.C., M.S.R.); and Section of Pharmacokinetics, Department of Pharmacology, Martin Luther University Halle-Wittenberg, Halle, Germany (M.W.)

Received August 22, 2000; accepted January 12, 2001 This paper is available online at http://jpet.aspetjournals.org

ABSTRACT

This work studied the structure-hepatic disposition relationships for cationic drugs of varying lipophilicity using a single-pass, in situ rat liver preparation. The lipophilicity among the cationic drugs studied in this work is in the following order: diltiazem > propranolol > labetalol > prazosin > antipyrine > atenolol. Parameters characterizing the hepatic distribution and elimination kinetics of the drugs were estimated using the multiple indicator dilution method. The kinetic model used to describe drug transport (the "two-phase stochastic model") integrated cytoplasmic binding kinetics and belongs to the class of barrier-limited and space-distributed liver models. Hepatic extraction ratio (*E*) (0.30–0.92) increased with lipophilicity. The intracellular binding rate constant (k_{on}) and the equilibrium amount ratios characterizing the slowly and rapidly equilibrating binding sites (K_S and K_R) increase with the lipophilicity of drug (k_{on}: 0.05–0.35 s^{-1}; K_S: 0.61–16.67; K_R: 0.36–0.95), whereas the intracellular unbinding rate constant (k_{off}) decreases with the lipophilicity of drug (0.081–0.021 s^{-1}). The partition ratio of influx (k_{in}) and efflux rate constant (k_{out}), k_{in}/k_{out}, increases with increasing pK_a value of the drug [from 1.72 for antipyrine (pK_a = 1.45) to 9.76 for propranolol (pK_a = 9.45)], the differences in $k_{in/kout}$ for the different drugs mainly arising from ion trapping in the mitochondria and lysosomes. The value of intrinsic elimination clearance (CL_{int}), permeation clearance (CL_{pT}), and permeability-surface area product (*PS*) all increase with the lipophilicity of drug [CL_{int} (ml · min^{-1} · g^{-1} of liver): 10.08–67.41; CL_{pT} (ml · min^{-1} · g^{-1} of liver): 10.80–5.35; *PS* (ml · min^{-1} · g^{-1} of liver): 14.59–90.54]. It is concluded that cationic drug kinetics in the liver can be modeled using models that integrate the presence of cytoplasmic binding, a hepatocyte barrier, and a vascular transit density function.

The liver is the main organ in the body for the conversion of drugs, toxins, and body products into more water-soluble forms so as to facilitate excretion by the kidney and biliary system. Although the enzymes involved in this conversion have been widely studied, there is relatively limited information on how the liver transports drugs within its cells and why some drugs (e.g., propranolol) bind strongly to components in the cells.

This work is concerned with intrahepatocellular binding as a determinant of hepatic drug disposition, especially the "first pass effect". It is now known that, in the liver, α_1-acid glycoprotein (AAG) is a potentially important intrahepatocellular binding protein for cationic drugs (Mansor et al., 1991). Plasma concentrations of cationic drugs are often related to AAG concentrations, because these drugs normally bind strongly to AAG (Garrido et al., 2000).

Cationic drugs are of particular interest for a number of reasons: 1) they constitute 70 to 80% of all drugs (Steen et al., 1991; Moseley et al., 1992); 2) they often have a limited therapeutic ratio (e.g., cardiovascular, analgesic, and psychotherapeutic drugs); and 3) they constitute the majority of drugs showing a high first pass effect (Marzo, 1992; Tam, 1993). Many of the anticancer drugs are also cations (e.g., epirubicin). To our knowledge, this study is the first report to investigate the structure-hepatic disposition relationships for cationic drugs in the isolated perfused rat liver prepara-

This work was supported by the National Health and Medical Research Council of Australia and the Queensland and New South Wales Lions Kidney and Medical Research Foundation.

ABBREVIATIONS: AAG, α_1-acid glycoprotein; MID, multiple indicator dilution; *E*, hepatic extraction ratio; BSA, bovine serum albumin; MTT, mean transit time; CV^2, normalized variance; MOPS, 3-(*N*-morpholino)propanesulfonic acid; RBC, red blood cell; HPLC, high performance liquid chromatography; f_{uB}, fraction unbound in blood; k_{in}, influx rate constant; k_{out}, efflux rate constant; k_{on}, intracellular binding rate constant; k_{off}, intracellular unbinding rate constant; K_R, equilibrium amount ratio characterizing the rapidly equilibrating binding sites; K_S, equilibrium amount ratio characterizing the slowly equilibrating binding sites; CL_{int}, intrinsic elimination clearance; CL_{pT}, permeation clearance; V_B, extracellular reference space; V_C, cellular water volume; f_{uC}, fraction unbound in cells; *PS*, permeability-surface area product of the hepatocyte membrane to the solute; *Q*, perfusion flow rate.

tion. The results may lead to an understanding of the role played by intrahepatocellular binding of cationic drugs on their kinetics and trafficking within hepatocytes.

The structure-hepatic disposition relationships of model cationic drugs (atenolol, antipyrine, prazosin, labetalol, propranolol, and diltiazem) with varying lipophilicity (Table 1) were determined in isolated perfused rat liver preparations using multiple indicator dilution (MID) technique. The aim of this study was to relate parameters characterizing the hepatic distribution and elimination kinetics of cationic drugs to their lipophilicity. A heterogeneous (barrier-limited and space-distributed) transit time model was used to estimate the rate constants of hepatocellular influx, efflux, binding, and elimination for each solute. The model is in principle equivalent to the standard MID approach and has been successfully used to study the hepatocellular binding and disposition kinetics of diclofenac (Weiss et al., 2000). Model independent parameters (E, MTT, CV^2) were determined by moments analysis.

Materials and Methods

Chemicals

Atenolol {4-[2-hydroxy-3-[(1-methylethyl)amino]propoxy]benzeneacetamide}, antipyrine {1,2-dihydro-1,5-dimethyl-2-phenyl-3*H*-pyrazol-3-one}, prazosin {1-(4-amino-6,7-dimethoxy-2-quinazolinyl)-4-(2-furanylcarbonyl)piperazine}, labetalol {2-hydroxy-5-[1-hydroxy-2-[(1-methyl-3-phenylpropyl)amino]ethyl]benzamide}, propranolol {1-[(1-methylethyl)amino]-3-(1-naphthalenyloxy)-2-propanol}, and diltiazem {(2*S*-cis)-3-(acetyloxy)-5-[2-(dimethyl amino)ethyl]-2,3-dihydro-2-(4-methoxyphenyl)-1,5-benzo-thiazepin-4(5*H*)-one} were obtained from Sigma Chemical Co. (St. Louis, MO), and were used without any further purification. [U-^{14}C]Sucrose and [^{3}H]water were obtained from Amersham (Buckinghamshire, UK).

In Situ Rat Liver Perfusions

The in situ perfused rat liver preparation used in this study has been described previously (Cheung et al., 1996). Briefly, male Wistar rats (weighing 300 g approximately) were anesthetized by interperitoneal injection of xylazine 10 mg kg^{-1} (Bayer Australia, Pymble, NSW) and ketamine-hydrochloride 80 mg kg^{-1} (Parnell Laboratories Australia, Alexandria, NSW). Following laparotomy animals were heparinized (heparin sodium; David Bull Laboratories Australia, Mulgrave, Victoria, 200 units) via the inferior vena cava. The bile duct was cannulated with PE-10 (Clay Adams, Franklin Lakes, NJ). The portal vein was then cannulated using a 16-gauge intravenous catheter and the liver was perfused via this cannula with 2% BSA MOPS buffer (Blanchard, 1984), which contains 15% (v/v) prewashed canine red blood cells (RBCs) at pH 7.4, and oxygenated using a silastic tubing lung ventilated with 100% pure oxygen (BOC Gases Australia, North Ryde, NSW). The perfusion system used was nonrecirculating and used a peristaltic pump (Cole-Palmer, Vernon Hills, IL). After perfusion was effected the animals were sacrificed by thoracotomy and the thoracic inferior vena cava was cannulated with PE-240 (Clay Adams). The animal was placed in a temperature-controlled perfusion cabinet at 37°C. Liver viability was assessed by macroscopic appearance, bile production, oxygen consumption, and perfusion pressure as described by Cheung et al. (1996).

TABLE 1
The cationic drugs studied in this work and their physicochemical properties

Derivative	Empirical Formula	Mol. Wt.	Log P_{app} [a]	f_{uB} [b]	pK_a [c]
Atenolol	$C_{14}H_{22}N_2O_3$	266.34	0.14	0.74	9.60
Antipyrine	$C_{11}H_{12}N_2O$	188.22	0.33	0.60	1.45
Prazosin	$C_{19}H_{21}N_5O_4$	383.41	1.88	0.54	6.50
Labetalol	$C_{19}H_{24}N_2O_3$	328.41	2.69	0.52	7.40
Propranolol	$C_{16}H_{21}NO_2$	259.34	3.10	0.45	9.45
Diltiazem	$C_{22}H_{26}N_2O_4S$	414.52	3.53	0.28	7.70

Mol. Wt., molecular weight.
[a] Log P_{app} (octanol/water partition coefficient at pH 7.4) values from Mannhold et al. (1990), Moriguchi et al. (1994), Leo (1995), and Mannhold et al. (1998).
[b] Unbound fraction (f_{uB}) of model cationic drugs in 2% BSA MOPS buffer (pH 7.4), containing 15% (v/v) prewashed canine RBCs and incubated in a 37°C water bath for 30 min.
[c] pK_a (the negative logarithm of the ionisation constant) values from Hansch et al. (1990).

Bolus Studies

Perfusions were made at 15 ml/min in each liver. After a 10-min perfusion stabilization period, a solution (50 μl of perfusion medium) of a particular concentration of the cationic drug (4 mM atenolol/propranolol, 5 mM antipyrine, 3 mM prazosin/labetalol, 2 mM diltiazem approximately) containing [^{3}H]water (3×10^6 dpm) and [U-^{14}C]sucrose (1.5×10^6 dpm) was injected into the liver with outlet samples collected via a fraction collector over 4 min (1 s × 20, 4 s × 5, 10 s × 5, 30 s × 5). In each liver a maximum of six injections was made with the order of injection randomized and no repeat of the same injection in the same rat. A stabilization period of 10 min was afforded between two injections. The total perfusion time for each liver was less than 2 h. These samples were centrifuged and aliquots (100 μl) of supernatant (containing [^{3}H]water and [U-^{14}C]sucrose) were taken for scintillation counting using a MINAXI beta TRICARB 4000 series liquid scintillation counter (Packard Instruments, Meriden, CT). The residue was vortexed and prepared for high performance liquid chromatography (HPLC) analysis to determine the outflow concentration of each cationic drug.

Analytical Procedure

HPLC Instrumentation. HPLC generally used a system consisting of a Waters 616 Quaternary Pumping system (Waters, Milford, MA); a Waters 717-plus autoinjector; a Waters Symmetry C18 3.9 × 150-mm steel cartridge column; a Waters 474 fluorescence detector for atenolol, antipyrine, prazosin, labetalol, and propranolol detecting (excitation 300 nm/emission 375 nm); a Waters 996 PhotoDiode array detector monitoring at 210 nm for diltiazem detecting; and a Waters Millennium 2010 Chromatography Manager data system. The mobile phase used for atenolol, antipyrine, prazosin, labetalol, and propranolol was 100 mM KH_2PO_4 buffer with 25% acetonitrile, at pH 3.0 (flow rate 1.0 ml/min). The mobile phase used for diltiazem was 100 mM KH_2PO_4 buffer with 30% acetonitrile, at pH 5.1 (flow rate 1.0 ml/min). The mobile phase was filtered and degassed under vacuum through a Millipore HVLP 47-mm-diameter filter membrane with 0.45-μm pore size before use.

Extraction Procedure. The standards and samples (buffer with canine RBCs) were prepared for HPLC analysis according to the following extraction procedure. 1) Atenolol, antipyrine, prazosin, labetalol, and propranolol: 100-μl aliquots of sample were mixed with 25 μl of 20 mg/l pronethalol (internal standard) in methanol and 50 μl of 10% trichloroacetic acid in an Eppendorf tube. The tubes were vortexed for 1 min and centrifuged and 50 μl of the resulting supernatant was injected onto the column. 2) Diltiazem: 100-μl aliquots of sample were mixed with 100 μl of 5 mg/l desmethylimipramine (internal standard) and 500 μl of phosphate buffer (0.05 M KH_2PO_4, 0.05 M Na_2HPO_4, pH 7.5). The samples were extracted by shaking vigorously for 5 min with 9 ml of hexane: isoamyl alcohol (99:1) in a polypropylene tube. After centrifugation, the organic phase was pipetted to a 10-ml polypropylene tube, leaving at least 5-mm depth of organic phase to avoid getting contamination from the aqueous phase, and extracted by vortexing with 0.2 ml 0.05 M HCl for 1 min. After a further centrifugation, the organic phase was aspirated and injecting 100 μl of the resulting supernatant onto the column.

Calibration and Assay Validation. Calibration samples were obtained by dissolving particular cationic drug in methanol. Increasing amount of this methanolic solution was added to perfusate medium to generate calibration curves over the range of 0 to 5000 ng/ml. For all the drugs in this work, HPLC standard curves were linear within the range of concentrations studied, with linear regression analysis yielding r^2 values >0.999. The within-day coefficients of variation (CV) for the various cationic drugs were determined by establishing and running three separate standard curves on the same day. Identical unknown samples were also run and the exact concentration determined using the separated standard curves. The CV was determined by dividing the standard deviation of the determined unknown solute concentration by the mean of these concentrations. The within-day coefficients of variation for all the drugs studied in this work were within the range of 0.6 to 4.4% (n = 3). Detection limit (atenolol/antipyrine/labetalol = 50 ng/ml, prazosin = 25 ng/ml, propranolol = 5 ng/ml, diltiazem = 10 ng/ml) was established by injecting decreasing concentrations of particular cationic drug extracted standards (prepared in perfusate medium) onto the column.

Perfusion Medium Binding

These experiments were carried out in 2% BSA MOPS buffer (pH 7.4), which contains 15% (v/v) prewashed canine RBCs, and incubated at 37°C water bath for 30 min to attain the required temperature. A 500 μM solution of each cationic drug was prepared in this perfusate.

The unbound fraction (f_{uB}) of cationic drug was investigated using an ultra-filtration method. A 1.0-ml aliquot sample (in triplicate) was placed in an ultrafiltration tube (MPS-1, micro-partition system; Amicon, Beverly, MA) and centrifuged at 3000g for 10 min. The ultra-filtrate was then assayed by HPLC. The f_{uB} was determined as the ratio of the free concentration to total concentration of solute.

Data Analysis

The two-phase organ model, which describes intracapillary mixing, transfer across a permeability barrier, and the intracellular distribution and elimination kinetics (Weiss and Roberts, 1996; Weiss et al., 1997), was previously applied to the disposition of diclofenac in the isolated perfused rat liver assuming "slow" hepatocellular binding, i.e., reversible sequestration (Weiss et al., 2000). Here the model was used in a reparameterized form introducing an additional class of intracellular binding sites. Briefly, the model (Fig. 1) assumes drug transfer across the permeability barrier (plasma membrane) with influx and efflux rate constants k_{in} and k_{out}, respectively. The model recognizes that solute concentrations change in space and time in both phases. The stochastic approach represents the transit of a molecule through the organ as a series of sojourns in one of the two regions described by density functions. The distribution of successive sojourn times in the tissue region, i.e., the density of cellular residence times [$\hat{f}_y(s)$] describes the hepatocellular distribution and elimination kinetics. We started with the assumption of two cellular binding sites characterized by a rapid (R) and slow (S) dissociation process, respectively. In fitting the data we observed that the dissociation rate constant of the rapid process was extremely high. Thus, we simplified the model using the solution for $k_{off,\ R} \rightarrow \infty$, i.e., assuming an instantaneous equilibration process characterized by $K_R = k_{on,\ R}/k_{off,\ R,}$ the equilibrium amount ratio characterizing the rapidly equilibrating binding sites. (Note that "binding" is used for all of reversible sequestration processes into cellular pools or storage compartments.)

The sojourn time distribution $f_y(t)$ of a molecule after a single excursion in the cellular space for the resulting two-compartment cell model can be obtained by standard methods in the Laplace domain, $\hat{f}_y(s) = L^{-1}[f_y(t)]$, as described earlier (Weiss, 1999; Weiss et al., 2000):

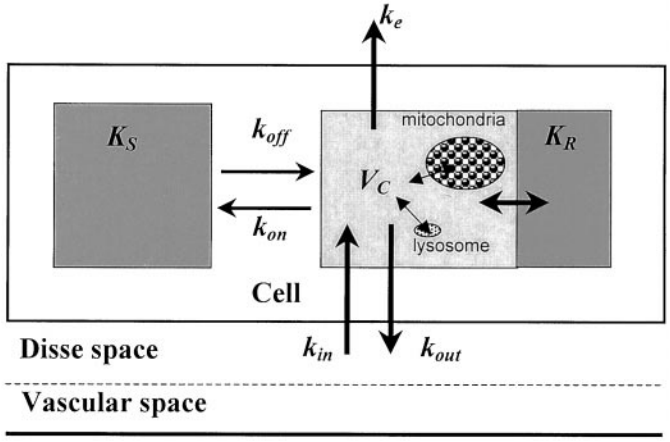

Fig. 1. Schematic overview of hepatocellular drug transport in the stochastic space-distributed liver model. k_{on} and k_{off} represent the intracellular binding and unbinding rate constant, respectively. K_S is the equilibrium amount ratio characterizing the slowly equilibrating binding sites. K_R is the equilibrium amount ratio characterizing the rapidly equilibrating binding sites. V_C is the cellular water volume. k_{in}, k_{out}, and k_e represent the permeation, efflux, and elimination rate constant, respectively. Also represented in the model are lysosomes and mitochondria, sites for ion trapping of cationic drugs.

$$\hat{f}_y(s) = \frac{(s + k_{off})k_{in}}{s^2(k_{in}/k_{out})(1 + K_R) + s((k_{in}/k_{out}) \cdot (k_{off} + K_R k_{off} + k_e + k_{on}) + k_{in}) + (k_{in}/k_{out})k_e k_{off} + k_{in}k_{off}} \quad (1)$$

where the permeation rate constant $k_{in} = CL_{pT}/V_B$ is the permeation clearance per extracellular volume V_B (note that $CL_{pT} = f_{uB}PS$; PS is the permeability-surface product, f_{uB} is the free fraction of solute in the perfusate), k_{on} and k_{off} representing the intracellular binding and unbinding rate constant, respectively, determining the equilibrium amount ratio $K_S = k_{on}/k_{off}$ characterizing the slowly accessible pool, and the elimination rate constant $k_e = CL_{int}/V_C$ is the intrinsic elimination clearance normalized per cellular volume V_C.

This approach is comparable with the liver MID model proposed by Schwab et al. (1990) and the model applied by Audi et al. (1998) to the isolated perfused rabbit lung assuming multiple intracellular binding sites. Note that due to the assumption of two intracellular storage compartments the definition of k_{on} and k_{off} differs from the model previously used for diclofenac (Weiss et al., 2000).

The transit time density function $\hat{f}(s)$ of drug molecules across the liver can then be derived in terms of the extracellular transit time density of nonpermeating reference molecules $\hat{f}(s)$ [in this study sucrose $\hat{f}_{sucr}(s)$], and the density function of successive sojourn times $\hat{f}_y(s)$ of the drug molecules into the cellular space:

$$\hat{f}(s) = \hat{f}_B[s + k_{in}(1 - \hat{f}_y(s))] \quad (2)$$

The fractional outflow versus time data were fitted in the time domain using a numerical inverse Laplace transformation of the appropriate transit time density function applying the nonlinear regression program SCIENTIST (MicroMath Scientific Software, Salt Lake City, UT). Data were analyzed by a sequential procedure. First, the fractional outflow curve $C_{sucr}(t)$ of the extracellular marker [U-^{14}C]sucrose was fitted by eq. 3, whereby $\hat{f}_{cath}(s)$ accounts for the catheter and $\hat{f}_B(s)$ includes the large vessel transit time:

$$C_{sucr}(t) = \frac{\text{Dose}}{Q} L^{-1}\{\hat{f}_{cath}(s)\hat{f}_B(s)\} \quad (3)$$

and the transit time density of the nonpermeating indicator is given by the following equation:

$$\hat{f}_B(s) = p\hat{f}_1(s) + (1 - p)\hat{f}_2(s) \quad (4)$$

with

$$\hat{f}_i(s) = \exp\left\{\frac{1}{CV_i^2} - \left[\frac{MT_i}{CV_i^2/2}\left(s + \frac{1}{2MT_iCV_i^2}\right)\right]^{1/2}\right\} (i = 1, 2) \quad (5)$$

Equation 5 is the Laplace transform of the inverse Gaussian density function with mean MT_i and relative dispersion CV_i^2. [It was shown previously that eqs. 3 through 5 adequately describe the transit time density of vascular markers in perfused rat livers (Weiss et al., 1997, 1998).]

The catheter transit time density was determined in the same way, i.e., by an independent experiment fitting eqs. 4 and 5 to the outflow profile of the catheter system. The four parameters describing $\hat{f}_{cath}(s)$ were then fixed in fitting the liver outflow data. It should be also noted that in contrast to the Goresky approach (Schwab et al., 1990) the delay due to the nonexchanging liver vessels (t_0) was not determined directly; however, the inverse Gaussian density accounts for a lag time (for $CV^2 \leq 1$ the apparent lag-time increases with decreasing values of CV^2; Weiss, 1997). This model, however, also corrects for the differences in the first appearance time of sucrose and water.

The mean transit time of the extracellular reference, $MTT_B = \int_0^\infty tf_B(t)dt$, is given by the following equation:

$$MTT_B = pMT_1 + (1 - p)MT_2 \quad (6)$$

$V_B = MTT_BQ(1 - \text{hematocrit})$, is the volume, accessible to sucrose, i.e., the sum of the sinusoidal plasma space and the Disse space, $V_B = V_{Plasma} + V_{Disse}$ [$Q(1 - \text{hematocrit})$ denotes the plasma flow rate]. Since sucrose does not distribute into erythrocytes, this extracellular space value has to be corrected for hematocrit (Varin and Huet 1985). Also, using this information the outflow concentration data of the permeating drugs, $C(t)$, were analyzed, i.e., the parameters MT_i, CV_i^2 (i = 1, 2), and p of the individual fits of [U-^{14}C]sucrose data were substituted as fixed parameters in $\hat{f}_B(s)$ of the model (eq. 2):

$$C(t) = \frac{\text{Dose}}{Q} L^{-1}\{\hat{f}_{cath}(s)\hat{f}(s)\} \quad (7)$$

and the parameters k_{in}, $k_{out,}$ k_{on}, k_{off}, K_R, and k_e were estimated.

The cellular distribution volume of water was estimated in the same way, i.e., by fitting the [^{3}H]water outflow data with eq. 7 using the density function for water $\hat{f}_W(s)$ instead of $\hat{f}(s)$. The latter differ only with regard to the respective tissue residence time densities $\hat{f}_y(s)$; assuming no cytoplasmic binding of water and $k_{out,\,w} = k_{in,\,w}v_{c,\,w}$ where $v_{c,\,w}$ denotes the normalized cellular water volume eq. 1 for well mixed intracellular distribution reduces (Weiss et al., 2000):

$$\hat{f}_{y,w}(s) = \frac{k_{in,w}/v_{c,w}}{k_{in,w}/v_{c,w} + s} \quad (8)$$

and is substituted in eqs. 2 and 7.

Nonparametric estimates of hepatic availability (F), mean transit time (MTT), and normalized variance (CV^2) were determined from the outflow concentration (C) versus time (t) profiles for the reference from eqs. 9 through 12 using the parabolas-through-the-origin method (extrapolated to infinity) with the assistance of the Moments Calculator 2.2 program for Macintosh computer (Purves, 1992).

$$F = \frac{Q \cdot AUC}{D} \quad (9)$$

$AUC = \int_0^\infty C(t)dt$ is the area under the solute concentration versus time curve, Q is the perfusate flow rate, and D is the dose of solute administered. All concentrations used were expressed in molar equivalents. Hepatic extraction ratio (E) equals to $1 - F$.

$$MTT = \frac{\int_0^\infty tC(t)dt}{AUC} \quad (10)$$

$$CV^2 = \frac{\sigma^2}{MTT^2} \quad (11)$$

where

$$\sigma^2 = \frac{\int_0^\infty t^2C(t)dt}{\int_0^\infty C(t)dt} - MTT^2 \quad (12)$$

Statistical Analysis

All data are presented as mean ± standard deviation unless otherwise stated. The model selection criterion provided by SCIENTIST, a modified Akaike Information Criterion (normalized to the number of data points), is defined by the following formula:

$$MSC = \ln\left[\frac{\sum_{i=1}^{n} w_i(C_{obs_i} - \bar{C}_{obs})^2}{\sum_{i=1}^{n} w_i(C_{obs_i} - C_{cal_i})^2}\right] - \frac{2p}{n} \quad (13)$$

where w_i are the weights applied to each concentration data point, n is the number of points, C_{obs_i} are the observed concentrations, C_{cal_i} are the values predicted by the model, $\bar{C}_{obs}$ is the weighted mean of the observed data, and p is the number of estimated parameters. This equation is used to compare the models with regard to "goodness of fit"; the most appropriate model, from a pure statistical point of view, is that with the largest model selection criterion. Information on parameter statistics was obtained from the approximate coefficients of variation of each estimate and the correlation matrix. A high coefficient of variation and/or correlation between parameters suggests unreliable estimates.

Results

The experimental parameters associated with the perfusion studies were (mean ± S.D., $n = 6$) rat weight = 298 ± 18 g, liver weight = 8.45 ± 1.24 g, bile flow = 1.54 ± 0.09 $\mu l \cdot min^{-1} \cdot g^{-1}$ of liver, oxygen consumption = 1.14 ± 0.12 $\mu mol \cdot min^{-1} \cdot g^{-1}$ of liver, and perfusion pressure = 11.45 ± 2.13 cm of H_2O. These values, reflecting liver viability, are comparable to those reported by Varin and Huet (1985) in a similar type of preparation.

The estimated model parameters for extracellular volume (determined by [U-^{14}C]sucrose), cellular volume (determined by [^{3}H]water), and ratio of cellular volume to extracellular volume were V_B = 0.49 ± 0.15 ml g^{-1} of liver, V_C = 1.30 ± 0.44 ml g^{-1} of liver, and v_c (V_C/V_B) = 2.65 ± 0.90 ($n = 6$), respectively. The value of v_c is in good agreement with the value of the fractional intracellular water space of 3.0 reported by Pang et al. (1988, 1990, 1991).

Figure 2 shows the typical outflow profile (logarithmic scale) and data fitting result (regression line) for [U-^{14}C]sucrose with the corresponding cationic drug. [U-^{14}C]Sucrose was coadministered as an extracellular reference solute with each cationic drug bolus injection. The fit was obtained by eqs. 3 to 5 for [U-^{14}C]sucrose and eqs. 1 to 7 for cationic drug.

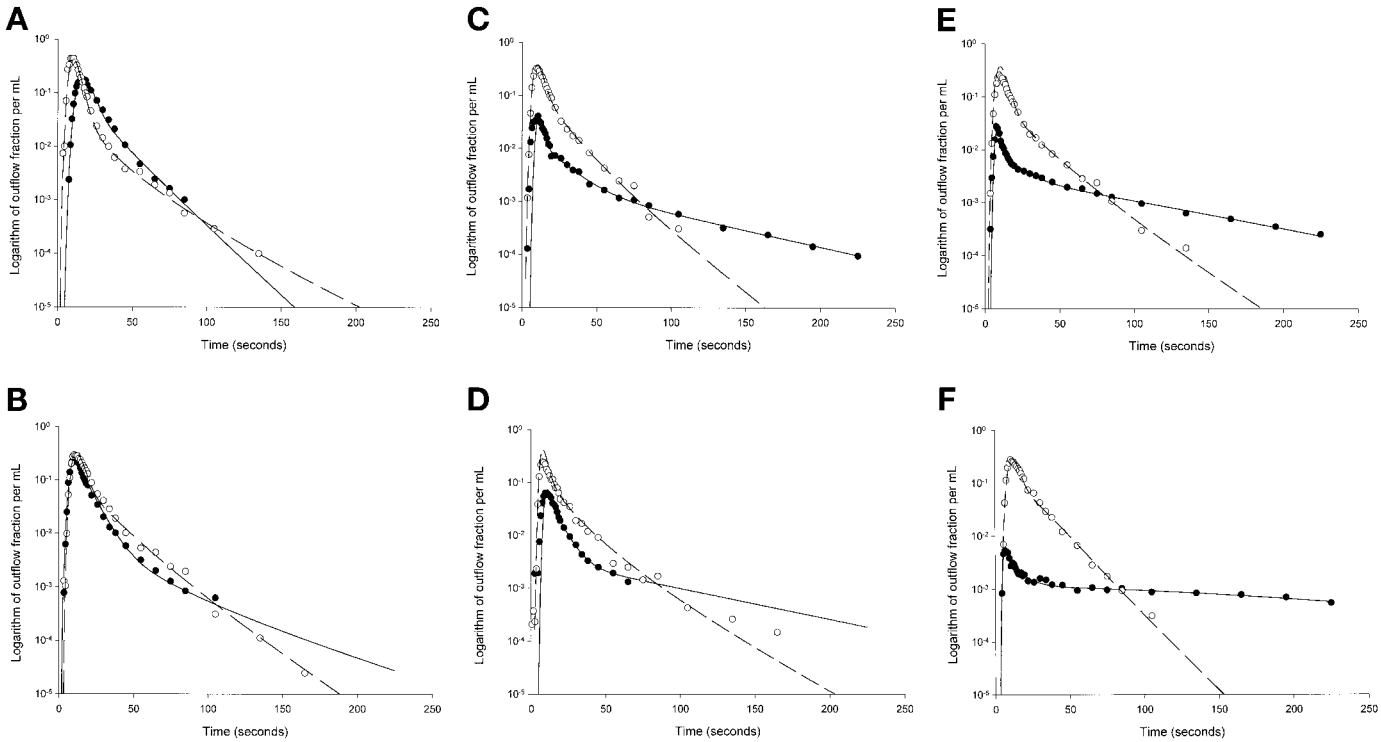

Fig. 2. Typical outflow profiles for the model cationic drugs and [U-^{14}C]sucrose (data weighted, $1/y_{obs}^2$) in the regressions. A, atenolol with sucrose; B, antipyrine with sucrose; C, prazosin with sucrose; D, labetalol with sucrose; E, propranolol with sucrose; and F, diltiazem with sucrose. The solid circles (●) represent cationic drug experimental data. The open circles (○) represent sucrose experimental data. The lines represent the fits of the profiles using eqs. 3 to 5 for [U-^{14}C]sucrose and eqs. 1 to 7 for cationic drugs.

It is apparent that this model fitted the data robustly. The more lipophilic the drug, the lower will be the peak high (higher hepatic extraction) and the slower decline will be the curve (longer mean transit time) for all cationic drugs studied in this work. The sucrose curves show a similar pattern among various bolus injections.

Table 1 presents the f_{uB}, molecular weight, log P_{app}, and pK_a values of model cationic drugs. It is apparent that f_{uB} decreases with increasing lipophilicity of drug.

Table 2 lists the results of nonparametric moments analysis for model cationic drugs studied in this work. It shows that the E value increases with the lipophilicity of drug [E = 0.255 + 0.191 log P_{app} (r^2 = 0.971), from 0.30 for atenolol to 0.92 for diltiazem]. The MTT value also increases with the lipophilicity of drug [MTT = 5.299 + 18.869 log P_{app} (r^2 = 0.645), from 14.34 s for atenolol to 105.32 s for diltiazem]. The CV[2] value for the drugs did not appear to be related to lipophilicity.

TABLE 2

Nonparametric moments results for model cationic drugs studied in this work (mean ± S.D., n = 6)

Drug	Log P_{app}[a]	E[b]	MTT[c]	CV[2 d]
			s	
Atenolol	0.14	0.30 ± 0.09	14.34 ± 2.73	0.64 ± 0.56
Antipyrine	0.33	0.30 ± 0.08	19.23 ± 2.28	0.34 ± 0.08
Prazosin	1.88	0.63 ± 0.01	26.62 ± 3.69	0.96 ± 0.31
Labetalol	2.69	0.69 ± 0.07	34.96 ± 1.79	0.19 ± 0.07
Propranolol	3.10	0.91 ± 0.04	51.52 ± 10.65	1.18 ± 0.33
Diltiazem	3.53	0.92 ± 0.02	105.32 ± 10.48	0.44 ± 0.11

[a] From Table 1.
[b] Hepatic extraction ratio (E) = 1 − hepatic availability (F) (E = 0.255 + 0.191 log P_{app}, r^2 = 0.971).
[c] Mean transit time (corrected for the catheter transit time).
[d] Normalized variance.

Table 3 summarizes the parameters estimated using the stochastic two-phase model of hepatic drug disposition. The k_{on} value increases significantly with the lipophilicity of drug [log k_{on} = −1.249 + 0.252 log P_{app} (r^2 = 0.944), from 0.05 s^{-1} for atenolol to 0.35 s^{-1} for diltiazem]. In contrast, the k_{off} value decreases with the lipophilicity of drug [log k_{off} = −1.012 − 0.185 log P_{app} (r^2 = 0.953), from 0.081 s^{-1} for atenolol to 0.021 s^{-1} for diltiazem]. The partition ratio of k_{in} and k_{out}, $k_{in/kout}$, increases with increasing pK_a value of the drug [log k_{in}/k_{out} = 0.079 + 0.091 pK_a (r^2 = 0.914), from 1.72 for antipyrine (pK_a = 1.45) to 9.76 for propranolol (pK_a = 9.45)]. The permeation and elimination kinetics parameters PS, CL_{pT}, and CL_{int} increase with the lipophilicity of drug [log PS = 1.180 + 0.183 log P_{app} (r^2 = 0.864), from 14.59 ml · min^{-1} · g^{-1} of liver for atenolol to 90.54 ml · min^{-1} · g^{-1} of liver for diltiazem; log CL_{pT} = 1.045 + 0.098 log P_{app} (r^2 = 0.899), from 10.80 ml · min^{-1} · g^{-1} of liver for atenolol to 25.35 ml · min^{-1} · g^{-1} of liver for diltiazem; log CL_{int} = 0.936 + 0.257 log P_{app} (r^2 = 0.993), from 10.08 ml · min^{-1} · g^{-1} of liver for atenolol to 67.41 ml · min^{-1} · g^{-1} of liver for diltiazem]. The steady-state distribution parameters K_S and K_R are also related to log P_{app} [log K_S = −0.239 + 0.438 log P_{app} (r^2 = 0.992), from 0.61 for atenolol to 16.67 for diltiazem; log K_R = −0.517 + 0.121 log P_{app} (r^2 = 0.769), from 0.36 for atenolol to 0.95 for diltiazem]. There is no significant difference in the V_C values (data not shown) determined from the water outflow data administered simultaneously with the cationic drugs, i.e., V_C was not affected by the drug injected.

Discussion

Barrier-limited tissue distribution is conventionally used in most organ models of solute disposition such as the two-

TABLE 3
Kinetic parameters derived from the two-phase stochastic model of drug transport fitting for model cationic drugs (mean ± S.D., n = 6)

Drug	Log P_{app} [a]	pK_a [b]	Kinetic Parameters							
			k_{in}/k_{out} [c]	k_{on} [d]	k_{off} [e]	K_S [f]	K_R [g]	CL_{int} [h]	CL_{pT} [i]	PS [j]
				s^{-1}	s^{-1}			$ml \cdot min^{-1} \cdot g^{-1}$ liver	$ml \cdot min^{-1} \cdot g^{-1}$ liver	$ml \cdot min^{-1} \cdot g^{-1}$ liver
Atenolol	0.14	9.60	8.00 ± 1.75	0.05 ± 0.01	0.081 ± 0.011	0.61 ± 0.11	0.36 ± 0.09	10.08 ± 1.55	10.80 ± 2.13	14.59 ± 2.25
Antipyrine	0.33	1.45	1.72 ± 0.73	0.07 ± 0.02	0.087 ± 0.023	0.81 ± 0.24	0.35 ± 0.11	9.45 ± 2.14	13.65 ± 1.33	22.75 ± 2.53
Prazosin	1.88	6.50	3.37 ± 1.13	0.23 ± 0.09	0.053 ± 0.009	4.31 ± 0.78	0.39 ± 0.12	27.09 ± 2.99	15.15 ± 1.89	28.06 ± 3.43
Labetalol	2.69	7.40	6.10 ± 1.07	0.30 ± 0.08	0.034 ± 0.010	8.80 ± 1.56	0.49 ± 0.15	45.36 ± 5.67	18.30 ± 2.34	35.19 ± 4.19
Propranolol	3.10	9.45	9.76 ± 2.60	0.33 ± 0.05	0.022 ± 0.005	15.05 ± 1.05	0.89 ± 0.07	52.92 ± 3.78	24.90 ± 1.99	55.33 ± 3.79
Diltiazem	3.53	7.70	7.35 ± 1.25	0.35 ± 0.11	0.021 ± 0.009	16.67 ± 2.45	0.95 ± 0.23	67.41 ± 6.41	25.35 ± 2.79	90.54 ± 6.51

[a,b] From Table 1.
[c] Partition ratio of influx and efflux rate constant ($\log k_{in}/k_{out} = 0.079 + 0.091\ pK_a$, $r^2 = 0.914$).
[d] Intracellular binding rate constant ($\log k_{on} = -1.249 + 0.252 \log P_{app}$, $r^2 = 0.944$).
[e] Intracellular unbinding rate constant ($\log k_{off} = -1.012 - 0.185 \log P_{app}$, $r^2 = 0.953$).
[f] Equilibrium amount ratio characterizing the slowly equilibrating binding sites ($\log K_S = -0.239 + 0.438 \log P_{app}$, $r^2 = 0.992$).
[g] Equilibrium amount ratio characterizing the rapidly equilibrating binding sites ($\log K_R = -0.517 + 0.121 \log P_{app}$, $r^2 = 0.769$).
[h] Intrinsic elimination clearance ($\log CL_{int} = 0.936 + 0.257 \log P_{app}$, $r^2 = 0.993$).
[i] Permeation clearance ($\log CL_{pT} = 1.045 + 0.098 \log P_{app}$, $r^2 = 0.899$).
[j] Permeability-surface area product ($\log PS = 1.180 + 0.183 \log P_{app}$, $r^2 = 0.864$).

compartment dispersion model (Roberts et al., 1988, 1990; Yano et al., 1989) and "Goresky" model (Goresky et al., 1973). However, it is well recognized that the two-compartment dispersion model inadequately describes the tail part of outflow curves (Schwab et al., 1990; Luxon and Weisiger, 1992; Pang et al., 1995; Weiss et al., 1997, 2000; Tirona et al., 1998). The two-phase stochastic model of drug transport (Weiss and Roberts, 1996; Weiss et al., 2000) was used in this work to integrate cytoplasmic binding kinetics into the conventional barrier-limited tissue distribution model. Consequently, this model perfectly fitted the data from the peak to the tail part of outflow curves. Audi et al. (1998) have used a similar approach to report the binding of cationic drugs in the isolated perfused lung. In general, models using vascular references as a basis for drug disposition in perfused organs are generally comparable but mathematically not identical. In addition to the two-phase stochastic model used in this work, other approaches include the Goresky model (Schwab et al., 1990), the "slow diffusion" model of Luxon and Weisiger (1992), the convection-dispersion model, and transit density functions (Roberts et al., 1988; Yano et al., 1989; Chou et al., 1995; Hung et al., 1998a,b; Roberts and Anissimov 1999; Roberts et al., 2000). Although an integrated cytoplasmic binding, barrier-limited, and two-phase stochastic distribution model was able to describe the drug kinetic data in the present work, an integrated slow diffusion (instead of "slow binding") model failed to fit our data. A comparison of alternative models of cytoplasmic drug distribution (slow binding versus slow diffusion) can be found elsewhere (Weiss, 1999; Weiss et al., 2000).

The present article has shown that the hepatic extraction ratio (E) values for model cationic drugs studied in this work increased with lipophilicity. We have also shown that a homologous series of *O*-acyl salicylate esters (Hung et al., 1998a) and diflunisal esters extraction also increased with lipophilicity (Hung et al., 1998b). The finding that the hepatic extraction of the cationic drug is dependent on lipophilicity is consistent with reports in the literature for various families of compounds. It is well recognized that hepatic extraction increases with lipophilicity for barbiturates (Yih and Van Rossum, 1977; Toon and Rowland, 1983; Hiura et al., 1984; Watari et al., 1988), tetracyclines (Toon and Rowland, 1979), β-adrenoceptor blocking agents (Hinderling et al., 1984), aminosteroidal neuromuscular blocking agents (Proost et al., 1997), phenolic compounds (Mellick and Roberts, 1999), and in general (Goldstein et al., 1974). However, Chou et al. (1993) reported that other than for *n*-pentyl 5-ethyl barbituric acid, the extraction of the barbiturates by the liver was negligible in a single-pass, in situ perfused rat liver preparation using RBC-free, protein-free perfusate. The difference in extraction between the work of Chou et al. (1993) and that of others may be due to the low flow rate of 15 ml/min and RBC-free perfusate used by Chou et al. (1993), being inadequate for maximal barbiturate extraction. Hickey et al. (1996) reported that oxygen supply played a vital role for propranolol extraction in the isolated perfused cirrhotic rat liver.

Both the permeation and intrinsic elimination clearances of liver CL_{pT} and CL_{int} increase with log P_{app} (Table 3). In general, hepatic extraction is a function of hepatic clearance (CL_{pT} and CL_{int}), hepatic permeability (PS), fraction unbound in the perfusate (f_{uB}), flow rate (Q), and vascular

dispersion (Roberts et al., 1988, 1990). Because CL_{pT} and CL_{int} increase with lipophilicity to a greater extent than f_{uB} decreases with lipophilicity with flow rate and vascular dispersion being constant, the observed increase in E with increasing the lipophilicity of drug is expected.

The logarithmic permeability-surface area product (log PS) is linearly related to log P_{app} (Fig. 3). This linear relationship is consistent with that first described by Chou et al. (1995) and extended by Mellick and Roberts (1999). The intercept in this study (1.18) is similar to that of 1.53 reported by Mellick and Roberts (1999). The slightly low slope found in this study (0.18) relative to that of 0.44 reported by Mellick and Roberts (1999) probably reflects the perfusion conditions used. This study used RBCs containing perfusate at 15 ml/min, whereas Mellick and Roberts (1999) used RBC-free perfusate at 30 ml/min.

The putative nature of the slowly equilibrating binding sites described in this work has yet to be determined. The model used in this work cannot distinguish between binding to cytosolic binding sites, binding sites on cellular membranes, entry into the matrix of intracellular organelles such as mitochondria and lysosomes, or dissolution in the lipid bilayer of cellular membranes (Proost et al., 1997). Figures 4 and 5 showed that log k_{on}, log K_S, and log K_R values are related to log P_{app}, consistent with binding to both the slowly and rapidly equilibrating binding sites being related to the lipophilicity of drug. The decrease in log k_{off} value with increasing lipophilicity of drug (Fig. 4) is consistent with the slow-equilibrating binding site being lipophilic. Accordingly, the equilibrium amount ratio characterizing the slowly equilibrating binding sites $K_S = k_{on}/k_{off}$ increases with drug lipophilicity, whereas the fraction of solute unbound in the cells (f_{uC}) decreases with increasing lipophilicity of drug. In summary, the extent of uptake of the various cationic drugs by the two binding sites (K_S, K_R) is greater for the more lipophilic drugs.

The ratio k_{in}/k_{out} is determined by the clearances into and out of the hepatocyte via the sinusoidal membrane and by the distribution spaces for the unbound cationic drugs between the hepatocyte and the perfusate. Given that uptake by binding sites has already been accounted for by the model, the increase in the k_{in}/k_{out} ratio for the various cationic drugs relative to antipyrine (1.72 ± 0.73) (which is un-ionized over the range of physiological pH values) is possibly a reflection of ion trapping or asymmetric transport. Such effects are expected to be greater for cationic drugs with higher pK_a values and, hence, a higher fraction ionized over the range of physiological pH values. Figure 6 showed that log k_{in}/k_{out} values for the cationic drugs increased with increasing pK_a value of the drug, suggesting that ion trapping or asymmetric transport may be involved.

An estimate of the extent of ion trapping may be obtained from the consideration of the pH values and fractional vol-

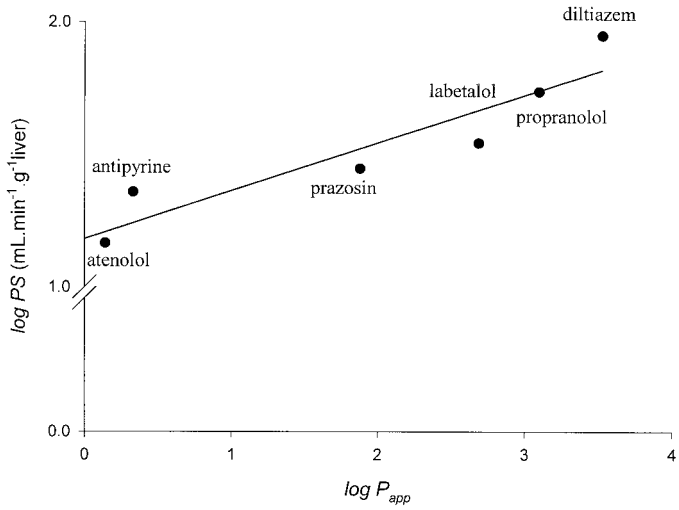

Fig. 3. Logarithmic relationship of permeability-surface area product (log PS, mean, $n = 6$) and lipophilicity (log P_{app}) for various cationic drugs. The line and solid circles (●) represent the log PS linear regression line (log $PS = 1.180 + 0.183 \log P_{app}$, $r^2 = 0.864$, $p < 0.05$) and data.

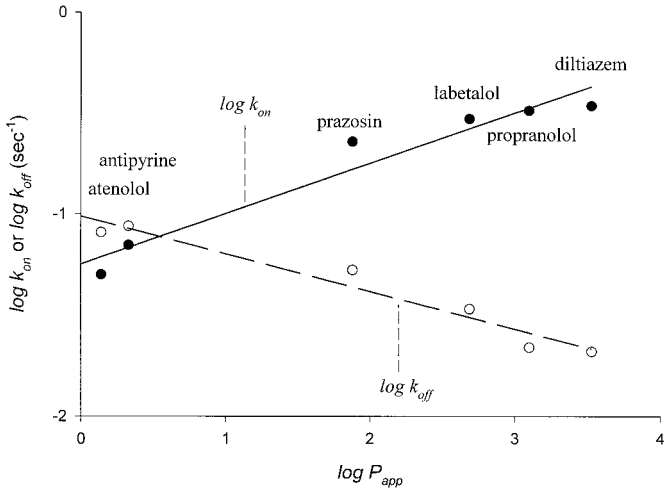

Fig. 4. Logarithmic relationship of intracellular binding rate constant (log k_{on}, mean, $n = 6$), intracellular unbinding rate constant (log k_{off}, mean, $n = 6$), and lipophilicity (log P_{app}) for various cationic drugs. The solid line and solid circles (●) represent the log k_{on} linear regression line (log $k_{on} = -1.249 + 0.252 \log P_{app}$, $r^2 = 0.944$, $p < 0.05$) and data. The long dash line and open circles (○) represent the log k_{off} linear regression line (log $k_{off} = -1.012–0.185 \log P_{app}$, $r^2 = 0.953$, $p < 0.05$) and data.

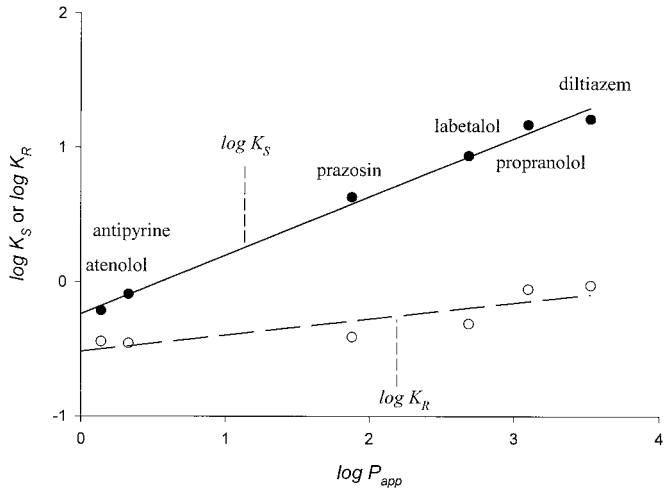

Fig. 5. Logarithmic relationship of equilibrium amount ratio characterizing the slowly equilibrating binding sites (log K_S, mean, $n = 6$), equilibrium amount ratio characterizing the rapidly equilibrating binding sites (log K_R, mean, $n = 6$), and lipophilicity (log P_{app}) for various cationic drugs. The solid line and solid circles (●) represent the log K_S linear regression line (log $K_S = -0.239 + 0.438 \log P_{app}$, $r^2 = 0.992$, $p < 0.01$) and data. The long dash line and open circles (○) represent the log K_R linear regression line (log $K_R = -0.517 + 0.121 \log P_{app}$, $r^2 = 0.769$) and data.

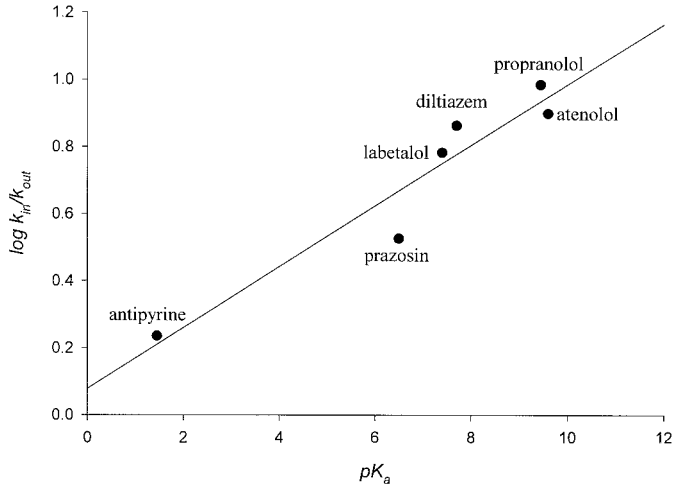

Fig. 6. Logarithmic relationship of partition ratio of influx and efflux rate constant (log k_{in}/k_{out}, mean, $n = 6$) and pK_a (the negative logarithm of the ionization constant) for various cationic drugs. The line and solid circles (●) represent the log k_{in}/k_{out} linear regression line (log $k_{in}/k_{out} = 0.079 + 0.091$ pK_a, $r^2 = 0.914$, $p < 0.05$) and data.

umes of the various cellular components, assuming that distribution is instantaneous and the resulting steady-state ratios are reflected in the observed ratios from dynamic (nonsteady-state) studies. When the unbound drug concentration is assumed to be identical in both the intracellular and perfusate compartments, the intracellular-to-perfusate concentration ratio for a drug with a given pK_a is given by $(1 + 10^{pK_a - pHi})/(1 + 10^{pK_a - pHp})$ (Goldstein et al., 1974), where pHi is the intracellular pH and pHp is the perfusate pH. In the simplest case, based on a perfused normal rat liver intracellular pHi of 7.27 (Le Couteur et al., 1993) and perfusate pHp of 7.4, then the concentration ratios for the cationic drugs studied in this work ranged from 1 to 1.35 (Table 4), suggesting a maximum ion trapping of 35%. A more profound pH-partitioning ion-trapping effect will be apparent for cations partitioning into organelles such as mitochondria and lysosomes where pH values of 6.67 (fasted) (Soboll et al., 1980) and 4.70 (Myers et al., 1995), respectively, have been reported. Apparent steady-state mitochondria/perfusate and lysosomes/perfusate concentration ratios based on these pH values and assuming fractional cytoplasmic volumes of 1 and 20% for lysosomes and mitochondria, respectively (Rhoades and Pflanzer, 1996), are shown in Table 4. Using the k_{in}/k_{out} for antipyrine, a basic drug un-ionized under physiological conditions, the predicted overall unbound cytoplasmic-to-perfusate concentration ratios can be used to estimate a predicted k_{in}/k_{out} ratio for each cationic drug. The predicted k_{in}/k_{out} values are similar (and not statistically different) to the experimental ratios obtained for k_{in}/k_{out} (Table 4). It is recognized that the predicted k_{in}/k_{out} values are only approximate because a range pH values has been reported for intracellular pH (7.19–7.29) (Le Couteur et al., 1993; Burns et al., 1999; Pietri et al., 2001), mitochondria pH (6.7–7.0) (Soboll et al., 1980), and lysosomal pH (4–5) (MacIntyre and Cutler, 1988; Myers et al., 1995; Proost et al., 1997) as well as differing lysosomal fractional volumes (0.68–1%) (Weibel et al., 1969; Rhoades and Pflanzer, 1996). Interpretation of the ion-trapping effect may be further complicated by binding or aggregation of basic drugs in lysosomes (Ishizaki et al., 2000) and by asymmetric exchange, since the interior of a hepatocyte is negatively charged relative to the extracellular space. Asymmetric exchange may also occur across the sinusoidal membrane as a result of cation transport by one or more of the reported cationic transporters (Zhang et al., 1998). In summary, intracellular, mitochondria, lysosomes, and perfusate pH differences and respective volume fractions enable the differing k_{in}/k_{out} values for the cations to be partly accounted for by a pH-partitioning ion-trapping effect. However, overall, the contribution of k_{in}/k_{out} as an explanation of differences in cationic drug disposition in the liver is small. Lipophilicity differences tend to dominate as determinants of hepatic extraction as is evident in a comparison of the k_{in}/k_{out} values of 8.00 and 7.35 for atenolol and diltiazem (Table 3) to their overall hepatic extraction ratios (E) values of 0.3 and 0.92 for atenolol and diltiazem (Table 2), and their corresponding octanol-water partition coefficients of 0.14 and 3.53 for atenolol and diltiazem (Table 1), respectively.

It is concluded that the structure-hepatic disposition relationships for cationic drugs is characterized by transmembrane exchange (permeability barrier) and the cytoplasmic binding process. The outflow curves of model cationic drugs were well described by a two-phase stochastic model of drug

TABLE 4
Overall unbound cytoplasmic/perfusate distribution ratio and ratios for intracellular, lysosomes, and mitochondria to perfusate concentrations for model cationic drugs

Drug	pK_a[a]	Intracellular to Perfusate Concentration Ratio (i:p)[b]	Lysosomes to Perfusate Concentration Ratio (l:p)[c]	Mitochondria to Perfusate Concentration Ratio (m:p)[d]	Overall Unbound Cytoplasmic/Perfusate Distribution Ratio (c:p)[e]	Predicted k_{in}/k_{out}[f]	Experimental k_{in}/k_{out}[g]
Atenolol	9.60	1.35	498.05	5.34	7.11	12.23	8.00 ± 1.75
Antipyrine	1.45	1.00	1.00	1.00	1.00	1.72	1.72 ± 0.73
Prazosin	6.50	1.04	56.93	1.49	1.69	2.91	3.37 ± 1.13
Labetalol	7.40	1.17	251.09	3.19	4.08	7.02	6.10 ± 1.07
Propranolol	9.45	1.35	496.77	5.33	7.10	12.21	9.76 ± 2.60
Diltiazem	7.70	1.23	334.19	3.91	5.10	8.77	7.35 ± 1.25

[a] From Table 1.
[b] Intracellular to perfusate concentration ratio = $(1 + 10^{pK_a - pHi})/(1 + 10^{pK_a - pHp})$ (Goldstein et al., 1974), where pHi = 7.27 is the intracellular pH (Le Couteur et al., 1993) and pHp = 7.40 is the perfusate pH.
[c,d] Using the same equation as footnote b.
[c] Where pHi = 4.70 is the lysosomes pH (Myers et al., 1995; Proost et al., 1997).
[d] Where pHi = 6.67 is the mitochondria pH in the fasted state (Soboll et al., 1980).
[e] Given that the fraction of lysosomes (f_{lys}) and mitochondria (f_{mito}) to cytosol is 1 and 20% (Rhoades and Pflanzer, 1996), the cytoplasmic/plasma distribution ratio (c:p) for model cationic drugs can be estimated from the individual organelle and remaining cytoplasmic volume fractions and concentration ratios above using the equation: c:p = $[f_{lys} \times$ l:p + $f_{mito} \times$ m:p + $(1 - f_{lys} - f_{mito}) \times$ i:p].
[f] Predicted k_{in}/k_{out} is given by c:p multiplied by 1.72, the k_{in}/k_{out} for antipyrine (Table 3), which is a cationic drug essentially un-ionized at pH values 4.7 to 7.4.
[g] Ratios of k_{in}/k_{out} from Table 3.

transport. The parameters E and MTT derived from moments increase with the lipophilicity of drug, whereas CV^2 did not differ significantly for any of the drugs studied in this work. In general, lipophilic drugs also have lower f_{uB} values. The derived pharmacokinetic parameters k_{on}, K_S, K_R, CL_{int}, CL_{pT}, and PS values increased with log P_{app}, whereas k_{off} value decreased with log P_{app} and V_C remained constant. Hence, increasing the lipophilicity of a cationic drug leads to a greater retention in the liver due to a more rapid uptake into the liver (higher PS), higher cytoplasmic binding, and slower dissociation rate off binding sites. However, the more lipophilic solutes are also associated with a higher permeation and intrinsic elimination clearance in the liver.

Acknowledgments

We are grateful to one of the referees whose comments greatly assisted the development of the section on ion trapping.

References

Audi SH, Dawson CA, Linehan JH, Krenz GS, Ahlf SB and Roerig DL (1998) Pulmonary disposition of lipophilic amine compounds in the isolated perfused rabbit lung. *J Appl Physiol* **84:**516–530.

Blanchard JS (1984) Buffers for enzymes. *Methods Enzymol* **104:**461.

Burns SP, Cohen RD, Iles RA, Bailey RA, Desai M, Germain JP and Going TCH (1999) Zonation of gluconeogenesis, ketogenesis and intracellular pH in livers from normal and diabetic ketoacidotic rats: evidence for intralobular redistribution of metabolic events in ketoacidosis. *Biochem J* **343:**273–280.

Cheung K, Hickman PE, Potter JM, Walker N, Jericho M, Haslam R and Roberts MS (1996) An optimised model for rat liver perfusion studies. *J Surg Res* **66:**81–89.

Chou CH, Evans AM, Fornasini G and Rowland M (1993) Relationship between lipophilicity and hepatic dispersion and distribution for a homologous series of barbiturates in the isolated perfused in situ rat liver. *Drug Metab Dispos* **21:**933–938.

Chou CH, McLachlan AJ and Rowland M (1995) Membrane permeability and lipophilicity in the isolated perfused rat liver: 5-ethyl barbituric acid and other compounds. *J Pharmacol Exp Ther* **275:**933–940.

Garrido MJ, Aguirre C, Troconiz IF, Marot M, Valle M, Zamacona MK and Calvo R (2000) Alpha 1-acid glycoprotein (AAG) and serum protein binding of methadone in heroin addicts with abstinence syndrome. *Int J Clin Pharmacol Ther* **38:**35–40.

Goldstein A, Aronow L and Kalman SM (1974) Principles of drug action, in *The Basis of Pharmacology*, 2nd ed., pp 146, 227–300, John Wiley & Sons, New York.

Goresky CA, Bach GC and Nadeau BE (1973) On the uptake of materials by the intact liver. The transport and net removal of galactose. *J Clin Invest* **52:**991–1009.

Hansch C, Sammes PG and Taylor JB (1990) *Comprehensive Medical Chemistry Vol. 6*: *Cumulative Subject Index & Drug Compendium*, pp 283, 288, 453, 613, 796, 810, Pergamon Press, New York.

Hickey PL, McLean AJ, Angus PW, Choo EF and Morgan DJ (1996) Increased sensitivity of propranolol clearance to reduced oxygen delivery in the isolated perfused cirrhotic rat liver. *Gastroenterology* **111:**1039–1048.

Hinderling PH, Schmidlin O and Seydel JK (1984) Quantitative relationships between structure and pharmacokinetics of beta-adrenoceptor blocking agents in man. *J Pharmacokinet Biopharm* **12:**263–287.

Hiura M, Nakagawa S, Kawashima H and Kaneniwa N (1984) Effect of lipid solubility on hepatic first pass metabolism of barbiturates in rabbits. *Int J Pharm* **20:**73–85.

Hung DY, Mellick GD, Anissimov YG, Weiss M and Roberts MS (1998a) Hepatic structure-pharmacokinetic relationships: the hepatic disposition and metabolite kinetics of a homologous series of O-acyl derivatives of salicylic acid. *Br J Pharmacol* **124:**1475–1483.

Hung DY, Mellick GD, Anissimov YG, Weiss M and Roberts MS (1998b) The hepatic disposition and metabolite kinetics of a homologous series of diflunisal esters. *J Pharm Sci* **87:**943–951.

Ishizaki J, Yokogawa K, Ichimura F and Ohkuma S (2000) Uptake of imipramine in rat liver lysosomes in vitro and its inhibition by basic drugs. *J Pharmacol Exp Ther* **294:**1088–1098.

Le Couteur DG, Rivory LP and Pond SM (1993) Hepatic intracellular pH during the prereplicative period following partial hepatectomy. *Am J Physiol* **264:**G767–G773.

Leo AJ (1995) Critique of recent comparison of logP calculation methods. *Chem Pharm Bull* **43:**512.

Luxon BA and Weisiger RA (1992) A new method for quantitating intracellular transport: application to the thyroid hormone 3,5,3′-triiodothyronine. *Am J Physiol* **263:**G733–G741.

Mannhold R, Cruciani G, Dross K and Rekker R (1998) Multivariate analysis of experimental and computational descriptors of molecular lipophilicity. *J Comput Aided Mol Des* **12:**573–581.

Mannhold R, Dross KP and Rekker RF (1990) Drug lipophilicity in QSAR practice. I. A comparison of experimental with calculative approaches. *Quant Struct Act Relat* **9:**21.

Mansor SM, Ward SA, Edwards G, Hoaksey PE and Breckenridge AM (1991) The influence of alpha 1-acid glycoprotein on quinine and quinidine disposition in the rat isolated perfused liver preparation. *J Pharm Pharmacol* **43:**650–654.

Marzo A (1992) Metabolism of drugs: a reappraisal. *Boll Chim Farm* **131:**139–143.

MacIntyre AC and Cutler DJ (1988) The potential role of lysosomes in tissue distribution of weak bases. *Biopharm Drug Dispos* **9:**513–526.

Mellick GD and Roberts MS (1999) Structure-hepatic disposition relationships for phenolic compounds. *Toxicol Appl Pharmacol* **158:**50–60.

Moriguchi I, Hirono S, Nakagome I and Hirano H (1994) Comparison of reliability of log P values for drugs calculated by several methods. *Chem Pharm Bull* **42:**976–978.

Moseley RH, Jarose SM and Permoad P (1992) Organic cation transport by rat liver plasma membrane vesicles: studies with tetraethylammonium. *Am J Physiol* **263:**G775–G785.

Myers BM, Tietz PS, Tarara JE and LaRusso NF (1995) Dynamic measurements of the acute and chronic effects of lysosomotropic agents on hepatocyte lysosomal pH using flow cytometry. *Hepatology* **22:**1519–1526.

Pang KS, Barker F III, Schwab AJ and Goresky CA (1990) [^{14}C]urea and ^{58}Co-EDTA as reference indicators in hepatic multiple indicator dilution studies. *Am J Physiol* **259:**G32–G40.

Pang KS, Barker F, Simard A, Schwab AJ and Goresky CA (1995) Sulfation of acetaminophen by the perfused rat liver: the effect of red blood cell carriage. *Hepatology* **22:**267–282.

Pang KS, Lee WF, Cherry WF, Yuen V, Accaputo J, Fayz S, Schwab AJ and Goresky CA (1988) Effects of perfusate flow rate on measured blood volume, Disse space, intracellular water space, and drug extraction in the perfused rat liver preparation: characterization by the multiple indicator dilution technique. *J Pharmacokinet Biopharm* **16:**595–632.

Pang KS, Xu N and Goresky CA (1991) D_2O as a substitute for ^3H_2O, as a reference indicator in liver multiple-indicator dilution studies. *Am J Physiol* **261:**G929–G936.

Pietri S, Martel S, Culcasi M, Delmas-Beauvieux MC, Canioni P and Gallis JL (2001) Use of diethyl (2-methyl-pyrrolidin-2-yl)phosphonate (DEPMPH) as a highly sensitive extra- and intracellular 31P NMR pH indicator in isolated organs. Direct NMR evidence of acidic compartments in the ischemic and reperfused rat liver. *J Biol Chem* **276:**1750–1758.

Proost JH, Roggeveld J, Wierda JM and Meijer DK (1997) Relationship between chemical structure and physicochemical properties of series of bulky organic cations and their hepatic uptake and biliary excretion rates. *J Pharmacol Exp Ther* **282:**715–726.

Purves RD (1992) Optimum numerical integration methods for estimation of area-under-the-curve (AUC) and area-under-the-moment-curve (AUMC). *J Pharmacokinet Biopharm* **20:**211–226.

Roberts MS and Anissimov Y (1999) Modelling of hepatic elimination and organ distribution kinetics with the extended convection-dispersion model. *J Pharmacokinet Biopharm* **27:**343–382.

Roberts MS, Anissimov YA and Weiss M (2000) Using the convection-dispersion model and transit density functions in the analysis of organ distribution kinetics. *J Pharm Sci* **89:**1579–1586.

Roberts MS, Donaldson JD and Rowland M (1988) Models of hepatic elimination: comparison of stochastic models to describe residence time distributions and to predict the influence of drug distribution, enzyme heterogeneity, and systemic recycling of hepatic elimination. *J Pharmacokinet Biopharm* **16:**41–83.

Roberts MS, Fraser S, Wagner A and McLeod L (1990) Residence time distributions of solutes in the perfused rat liver using a dispersion model of hepatic elimination: 1. effect of changes in perfusate flow and albumin concentration on sucrose and taurocholate. *J Pharmacokinet Biopharm* **18:**209–234.

Rhoades R and Pflanzer R (1996) *Human Physiology*, 3rd ed., pp 85 and 88, Harcourt Brace College Publishers, Philadelphia, PA.

Schwab AJ, Barker F III, Goresky CA and Pang KS (1990) Transfer of enalaprilat across rat liver cell membranes is barrier-limited. *Am J Physiol* **258:**G461–G475.

Soboll S, Elbers R, Scholz R and Heldt HW (1980) Subcellular distribution of di- and tricarboxylates and pH gradients in perfused rat liver. *Hoppe Seylers Z Physiol Chem* **361:**69–76.

Steen H, Oosting R and Meijer DK (1991) Mechanisms for the uptake of cationic drugs by the liver: a study with tributylmethylammonium (TBuMA). *J Pharmacol Exp Ther* **258:**537–543.

Tam YK (1993) Individual variation in first-pass metabolism. *Clin Pharmacokinet* **25:**300–328.

Tirona RG, Schwab AJ, Geng W and Pang KS (1998) Hepatic clearance models. Comparison of the dispersion and Goresky models in outflow profiles from multiple indicator rat liver studies. *Drug Metab Dispos* **26:**465–475.

Toon S and Rowland M (1979) Quantitative structure pharmacokinetic activity relationships with some tetracyclines. *J Pharm Pharmacol* **31 (Suppl):**P43.

Toon S and Rowland M (1983) Structure-pharmacokinetic relationships among the barbiturates in the rat. *J Pharmacol Exp Ther* **225:**752–763.

Varin F and Huet PM (1985) Hepatic microcirculation in the perfused cirrhotic rat liver. *J Clin Invest* **76:**1904–1912.

Watari N, Sugiyama Y, Kaneniwa N and Hiura M (1988) Prediction of hepatic first pass metabolism and plasma levels following intravenous and oral administration of barbiturates in the rabbit based on quantitative structure-pharmacokinetic relationships. *J Pharmacokinet Biopharm* **16:**279–301.

Weibel ER, Staubli W, Gnagi HR and Hess FA (1969) Correlated morphometric and biochemical studies on the liver cell. I. Morphometric model, stereologic methods, and normal morphometric data for rat liver. *J Cell Biol* **42:**68–91.

Weiss M (1997) On the degree of solute mixing in liver models of drug elimination. *J Pharmacokinet Biopharm* **25:**363–375.

Weiss M (1999) Cellular pharmacokinetics: effects of cytoplasmic diffusion and binding on organ transit time distribution. *J Pharmacokinet Biopharm* **27:**233–255.

Weiss M, Ballinger LN and Roberts MS (1998) Kinetic analysis of vascular marker distribution in perfused rat livers after regeneration following partial hepatectomy. *J Hepatol* **29:**476–481.

Weiss M, Kuhlmann O, Hung DY and Roberts MS (2000) Cytoplasmic binding and disposition kinetics of diclofenac in the isolated perfused rat liver. *Br J Pharmacol* **130:**1331–1338.

Weiss M and Roberts MS (1996) Tissue distribution kinetics as determinant of transit time dispersion of drugs in organs: application of a stochastic model to the rat hindlimb. *J Pharmacokinet Biopharm* **24:**173–196.

Weiss M, Stedtler C and Roberts MS (1997) On the validity of the dispersion model of hepatic drug elimination when intravascular transit time densities are long-tailed. *Bull Math Biol* **59:**911–929.

Yano Y, Yamaoka K, Aoyama Y and Tanaka H (1989) Two-compartment dispersion model for analysis of organ perfusion system of drugs by fast inverse Laplace transform (FILT). *J Pharmacokinet Biopharm* **17:**179–202.

Yih TD and Van Rossum JM (1977) Ka values of some homologous series barbiturates and the relationship with lipophilicity and metabolic clearance. *Biochem Pharmacol* **26:**2117–2120.

Zhang L, Brett C and Giacomini KM (1998) Role of organic cation transporters in drug absorption and elimination. *Annu Rev Pharmacol Toxicol* **38:**431–460.

Send reprint requests to: Professor Michael S. Roberts, Department of Medicine, University of Queensland, Princess Alexandra Hospital, Woolloongabba, Qld 4102, Australia. E-mail: M.Roberts@mailbox.uq.edu.au